IJSRM
INTERNATIONAL JOURNAL OF SCIENCE AND RESEARCH METHODOLOGY
An Official Publication of Human Journals

Human Journals
Research Article
October 2016 Vol.:4, Issue:4

Feasible Design of Wearable Tactile Sensation Device

IJSRM
INTERNATIONAL JOURNAL OF SCIENCE AND RESEARCH METHODOLOGY
An Official Publication of Human Journals

Takehiro Adachi[*1], Yasuyoshi Matsumoto[*1], Yoichi Hoshi[*2] and Junji Sone[*2]

**1 Department of Electronics and Information Technology, Graduate School of Engineering, Tokyo Polytechnic University, Japan.*

**2Faculty of Engineering, Tokyo Polytechnic University, Japan.*

Submission: 10 October 2016
Accepted: 15 October 2016
Published: 25 October 2016

Keywords: Tactile Sensation, Design, Simulation, Piezoelectric actuator

ABSTRACT

In this study, we considered a wearable tactile device. This device was composed of an interface part fabricated by 3D printing, pins, and cantilever-type actuators. The device was compact and had the ability to stimulate the mechanoreceptors of the fingertips. We used deformation finite element analysis to design multi-tile and multi-layer cantilever-type actuators for achieving the required displacement with piezoelectric actuators. This device could stimulate within the double-point threshold of the fingertips.

HUMAN JOURNALS
www.ijsrm.humanjournals.com

1. INTRODUCTION

Tactile feedback and force feedback are important for surgical systems [1] and tele-operated tasks [2]. We succeeded in presenting a force profile similar to that of real cutting [3]. There are many products for Braille display [4], and tactile devices have been researched [5]. A tactile display requires high density and high response to realizing the teleoperation and virtual reality that Braille code displays.

One of these tactile displays was realized using a magnetic micro-actuator that was based on a PDMS elastomer [6]. Although it could realize high density and high speed, its force was rather weak. Ion conducting polymer gel film actuators can realize high-density and high-speed display under wet conditions [7]. Watanabe and Miki developed a hydraulic displacement amplification mechanism that achieved large displacement using a micro-electromechanical system (MEMS) actuator and flexible micro-chamber filled with incompressible liquid [8]. The resolution was not sufficiently good for tactile sensation, but the large displacement achieved a high Braille code display capability. A shape memory alloy actuator is one possible solution [9, 10] but does not have sufficient response speed for use in a tactile device. Paschew and Richter developed a high-resolution display using smart hydrogel [11]. They used smart hydrogel as an actuator with temperature as the drive source, but the response time was not very fast. A similar polymer actuator was developed by Choi using a dielectric elastomer [12]. This resulted in a soft, flexible, and thin actuator, which could also be used as a wearable device. Ultrasound vibrators can also generate an artificial tactile sensation [13, 14]. A quasi-tactile device was developed using an electro tactile display. It is an interesting phenomenon that the tactile sense changes with polarity [15]. Material stiffness was represented using smart fluid [16]. An air jet [17], suction force [18], and air pressure control have all been used in tactile displays [19, 20]. However, these devices are difficult to use as wearable devices.

We aim to develop a small, wearable tactile device that can represent actual touching and shape information. Therefore, we selected MEMS and 3D printing technologies. We selected a piezoelectric actuator and carbon fiber-reinforced plastic (CFRP) stimulus pins. This was similar to Smithmaitrie's research [21], but we used MEMS technology. This report describes the feasibility of a tactile display. The deformation of a piezoelectric micro-actuator is small [22]; thus, we considered a method for larger deformation. In the second section, we describe

the concept of wearing the device, and in the third section, we explain the design method and results of the piezoelectric micro-actuator.

2. Concept of Wearing device

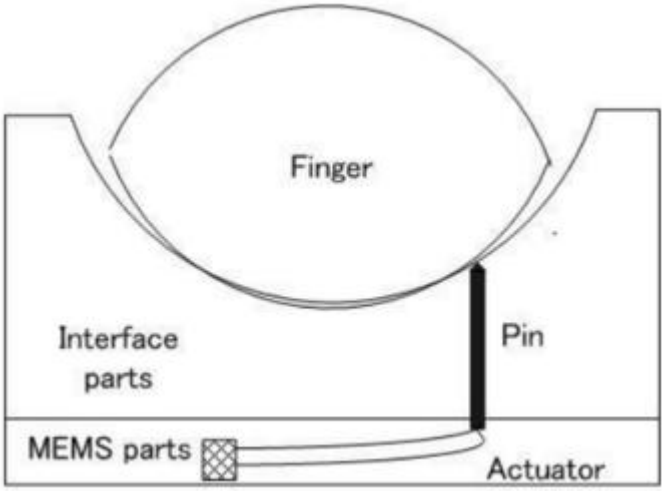

Figure. 1 Scheme of tactile device.

Figure 1 shows a schematic of our tactile device. A finger contacts the interface parts, and tactile sensation is generated by pins. The pins must be placed in high density, and CFRP is used. The interface parts are fabricated by 3D printing (we used ABS resin). The other parts are MEMS parts. Many actuators are disposed at high density in the interface parts, and each actuator is composed of a piezoelectric (lead zirconate titanate) cantilever. A piezoelectric cantilever actuator can move at high speed, and we can achieve a high-density actuator using MEMS technology. The double-point threshold is 2–3 mm at the fingertip; therefore; it is sufficient to set the pins at a distance of 2–3 mm within the array.

The finger and interface parts had to fit closely; therefore, we measured the main fingertip shape parameters of 100 men aged 20 to 54 years at the university. The parameters were: 1) Length of fingertip; 2) Width of fingertip at root; 3) Width of fingertip at top; 4) Radius of root; 5) Radius of top; 6) Section radius of root; 7) Section radius of top. Table 1 shows the average values of these parameters. We built the interface parts using these parameters. First, we made a 3D CAD model. We then fabricated the parts from the ABS material using a 3D printer. The nozzle hole diameter was 0.2 mm, and the layer pitch was 0.1 mm.

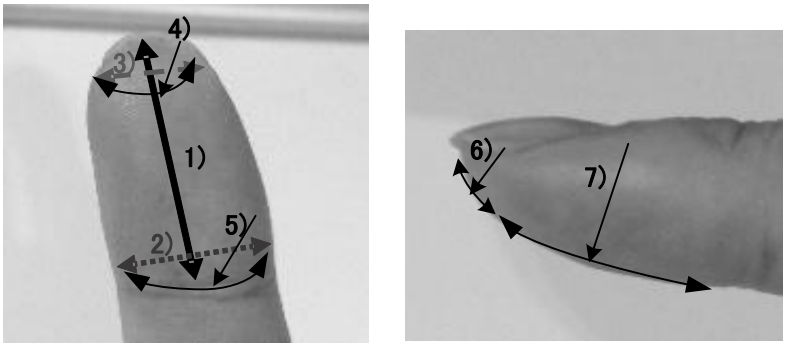

a) Plan view b) Side view

Figure 2. Parameters of fingertip shape.

Table 1 Measured result (Right hand-Index finger) (1)

[mm]	length of fingertip	With of fingertip at root,	Width of fingertip at top	Radius of root	Radius of top	Section radius of root	Section radius of top
Average data	25.84	14.49	11.83	17.83	13.38	21.70	12.93

3. Design of Piezoelectric Micro-actuator

3.1 Design method

(1) The stimulation targets were paciniform end-organs and Merkel cell neurite complexes. In this case, we needed to stimulate these mechanoreceptors by pressing to a 400-μm depth at the fingertips. Therefore, we designed the actuators to effect actuation to this depth. We then selected the following considerations:

(2) A cantilever was composed of many tiles aligned perpendicular to increase its length.

(3) A multilayer piezoelectric structure was used as a high-power drive.

(4) We used distortion of the width direction of the cantilever to increase the deformation.

(5) Cantilevers were placed closely to establish high-density stimulation points.

(6) Piezoelectric material Pb $(Zr,Ti)O_3$(PZT) was used for high-power actuation. The thickness of one layer was 3 μm.

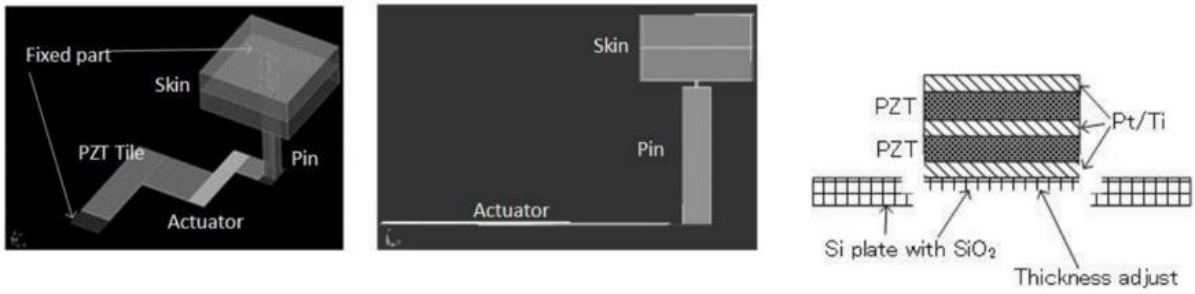

a) Isometric view b) Side view. c) Structure of actuator

Figure 3. Analysis model of cantilever, pin and human skin.

Figure 3 shows the analysis model. Four connected tiles compose the actuators, and each tile has a PZT multilayer and Si base layer. Each PZT layer has Pt electrodes, and drive and ground electrodes are placed alternately. The end of each actuator is connected to a CFRP pin, and the top of each pin is in contact with human skin. The top of each pin is a 0.5-mm square, which stimulates the fingertip. The human skin is 1 mm thick and its top plane is held in place by bone.

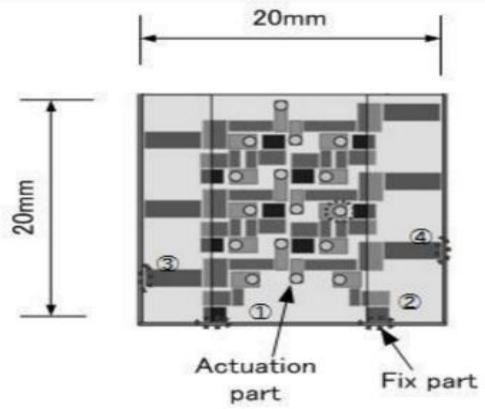

Figure 4. Cantilever layout result.

Figure 4 shows the cantilever layout result. To fabricate the wearable device, we used a 20-mm square Si plate, which was the overall device dimension, similar to the width and length of a fingertip. One side of a cantilever actuator was fixed, and another side was an actuation part, which connected to a stimulus pin. In this case, we aligned the stimulus pins within 2.5 mm. Table 2 shows the dimensions of each cantilever actuator. We prepared four types of actuators to establish high density, and each type of cantilever actuator had four tiles. Table 3 shows the material parameters. We used piezoelectric and deformation analysis using FEM software (MemsONE).

Table 2. The dimension of each cantilever actuators.

W×H [μm]	1 stage	2 stage	3 stage	4 stage
Model 1	640×2230	1070×960	350×1770	520×540
Model 2	790×420	1270×960	350×930	920×670
Model 3	4420×680	1120×810	4040×620	1330×400
Model 4	5390×780	2130×630	3530×500	1310×650

Table 3. Material parameters.

	Young ratio [kg/μ･m･s^2]	Poisson's ratio	Density [kg/μm^3]	Piezoelectric constant [s･A/μ･m^2]	Permittivity [s^4･A^2/kg･μ･m^3]
				e31,e32	E11,E22, E33
Si	1.65E5	2.20E-1	2.33E-15		
PZT	7.00E4	3.00E-4		8.26E-12	6.00E-27
CFRP	1.18E5	3.00E-1	1.53E-15		
Skin	1.36E-1	4.80E-1	9.38E-16		

3.2 Design results

(1) Relation between the thickness of the Si layer, displacement, and maximum principal stress.

We used 100 V for the drive voltage; the number of PZT layers was five; and the Si layer thicknesses were selected as 15, 25, 30, 35, 40, and 50 μm. Figure 5 shows the relation between the displacement of the pin tops and the Si thickness of each type of cantilever. Si thicknesses of 25 and 35 μm have large displacements for models 3 and 4. Figure 6 shows relation between the maximum principal stress and the Si thickness of each type of cantilever. From this result, the stiffness is insufficient for thicknesses less than 20 μm because of non-uniform deformation. Also, the Si part became very stiff, and the deformation of the cantilever was reduced by this increment of stiffness for thicknesses greater than 40 μm. The maximum principal stress was less than 500 MPa at Si thicknesses of 30 and 35 μm. This value was smaller than the fracture stress of Si.

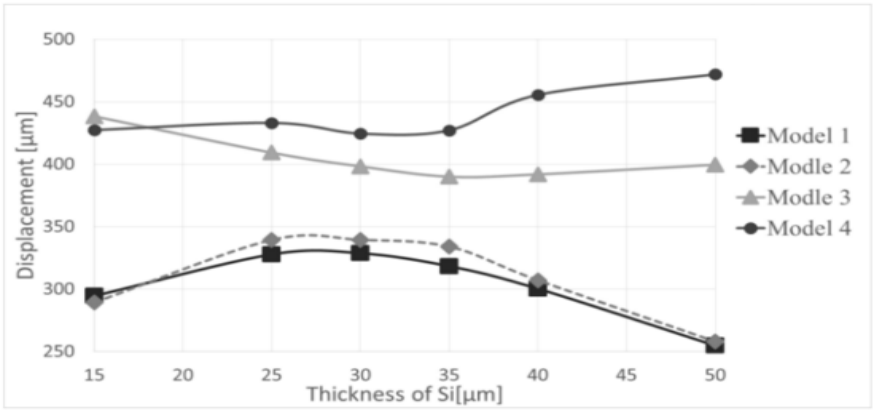

Figure 5. Relation between displacement of pins top and Si thickness of each type of cantilever.

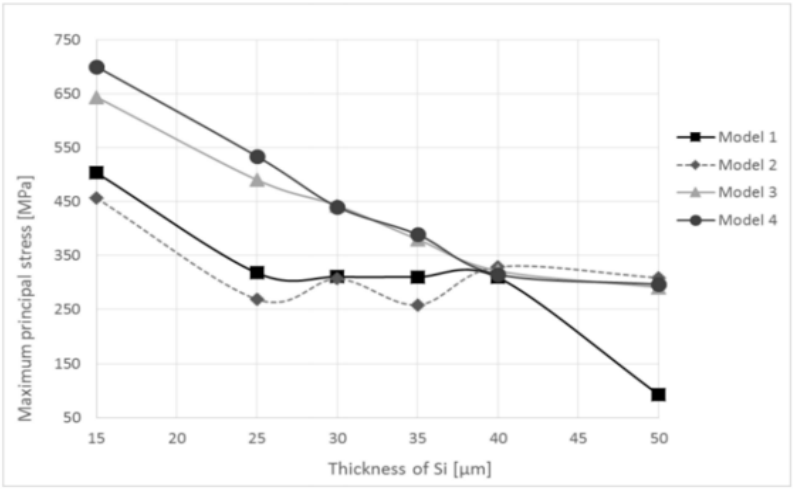

Figure 6. Relation between maximum principal stress and Si thickness of each type of cantilever.

(2) Relation between the number of PZT layers and the displacement of pins.

Figure 7 shows the relation between the displacement of pin tops and the number of PZT layers for each type of cantilever. From the results, Si thicknesses of 30 and 35 μm and nine PZT layers can achieve 400 μm of displacement for all models. Figure 8 shows relation between the maximum principal stress and the number of PZT layers for each type of cantilever. The Si thicknesses were selected as 30 and 35 μm. The maximum principal stress was reduced for a Si thickness of 35 μm. The maximum principal stress was 450 MPa for the nine layers of the PZT model 1 and 2. This value was less than the fracture stress of Si. The maximum principal stress of model 3 and 4 are exceeded 550MPa for model 3 and 4 for a Si thickness of 35 μm, displacements are 1.5 times larger than requirement for these model.

Therefore, drive voltage is reduced to 80V, this problem can be solved. From these analyses, our cantilever needs nine layers of PZT, and the thickness of the Si base must be 35 μm.

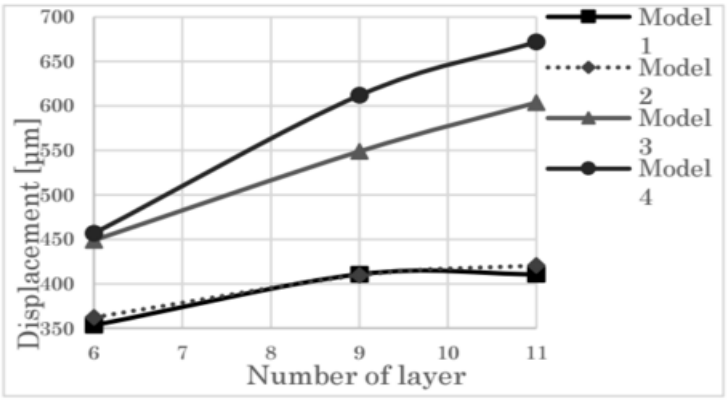

a) Case of Si thickness is 30μm.

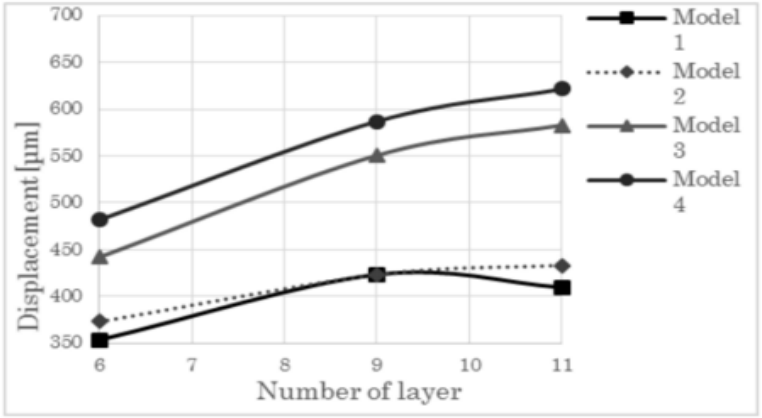

b) Case of Si thickness is 35μm.

Figure 7. Relation between displacement of pins top and number of layer of PZT for each type of cantilever.

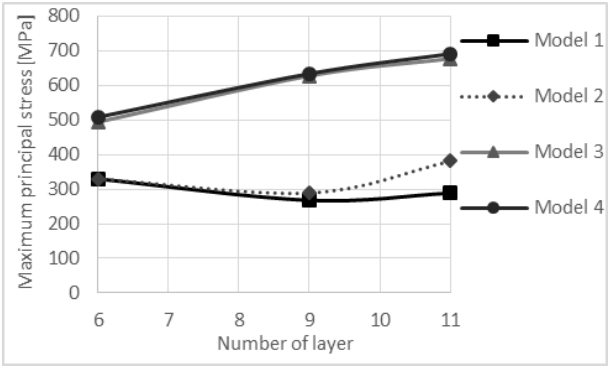

a) Case of Si thickness is 30μm.

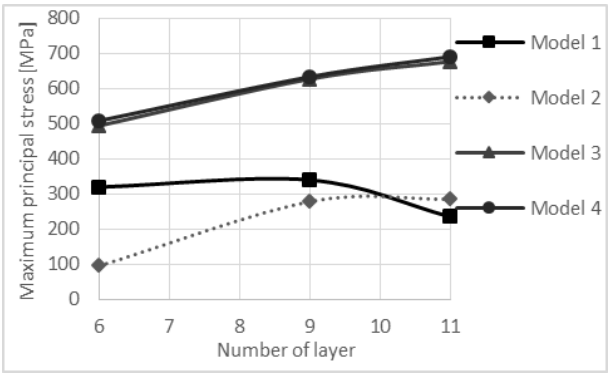

b) Case of Si thickness is 35μm.

Figure 8 Relation between maximum principal stress and number of layer of PZT for each type of cantilever.

(3) Interface parts printing result.

We made the interface parts using a 3D printer. Figure 9 shows results of the interface parts printing. It contains a MEMS part box, which holds the piezoelectric micro-actuators. The width is 33%, and the height is increased by 75% for fingertip sizes; thus, the restriction of finger movement is small. Therefore, we can realize a wearable tactile device.

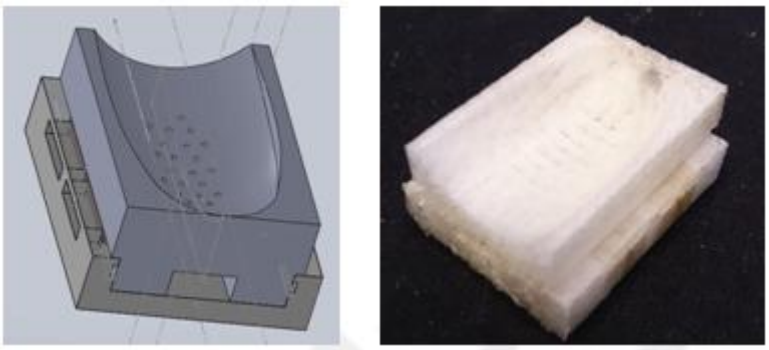

a) CAD model. b) Printed interface part.

Figure 9. Interface parts printing result.

3. CONCLUSION

We considered a wearable tactile display. Our device size is somewhat larger than a fingertip, and the limitation of fingertip movement is small. Our system can be used in various teleoperation tasks.

We designed four tile-connected cantilevers and a nine-layer piezoelectric actuator. This device can stimulate the mechanoreceptors of a fingertip. In addition, our tactile display can stimulate within the double-point threshold of a fingertip using a MEMS device simulation. Therefore, our system can display high-density information. If we add soft tissue onto the

skin analysis model, the displacement of the stimulating pins can be larger. This means that we can reduce the number of layers of the piezoelectric actuators.

As a next step, we plan to improve the finger model and the accuracy of the analysis. We will also make the MEMS parts using MEMS processing and confirm the performance of the actual device.

ACKNOWLEDGEMENT

A part of this work was supported by “Nanotechnology Platform” of the Ministry of Education, Culture, Sports, Science and Technology (MEXT), Japan, at the Center for Integrated Nanotechnology Support, Tohoku University and Tokyo University. This work was supported by JSPS KAKENHI Grant Number 15K12089. This work was one research of "Research and development of educational and communicational robot systems" approved by the Council for Promotion of Universal Future Society at MEXT, Japan.

REFERENCES

1) A. M. Okamura, L. N. Verner, C. E. Reiley, and M.Mahvash, Haptics for Robot-Assisted Minimally Invasive Surgery; Robotics Research, 66, (2011), 361-372.
2) M. K. O ’Malley and R. O. Ambrose: Haptic feedback applications for Robonaut, Industrial Robot, 30(6), (2003), 531-542.
3) J. Sone, K. Ogiwara, Y. Kume, Y. Tokuyama, M.Isobe, Force Profile study of Virtual Cutting, THE THIRTEENTH INTERNATIONAL CONFERENCE ON ARTIFICIAL REALITY AND TELEXISTENCE, (2003), 143-147.
4) Braille Technology, American Foundation for the Blind, http://www.afb.org/info/living-with-vision-loss/using-technology/assistive-technology/braille-technology/1235
5) H. Ishizuka, N. Miki, Review MEMS-based tactile displays, Displays 37, (2015), 25-32.
6) J. Streque, A. Talbi, P. Pernod, V. Preobrazhensky, New magnetic micro-actuator design based on PDMS elastomer and MEMS technologies for tactile display, IEEE Trans. Haptics 3 (2) ,(2010), 88-97.
7) M. Konyo, S. Tadokoro, T. Takamori, Artificial tactile feel display using soft gel actuators, in: Proceedings of the 2000 IEEE International Conference on Robotics and Automation, (2000), 3416-3422.
8) J. Watanabe, H. Ishikawa, X. Aroutte, Y. Matusumoto, N. Miki, Demonstration of vibrational braille code display using large displacement micro-electromechanical system actuators, Jpn. J. Appl. Phys. 51, (2012) , 06FL11-1-6.
9) F. Zhao, K. Fukuyama, H. Sawada, Compact Braille display using SMA wire array, in: Proceedings of the 18th IEEE International Symposium on Robot and Human Interactive Communication, (2009), 28-33.
10) L. Santos-Carreras, K. Leuenberger, P. Retornaz, R. Gassert, H. Bleuler, Design and psychophysical evaluation of a tactile pulse display for tele-operated artery palpation, in: Proceedings of the 2010 IEEE/RSJ International Conference on Intelligent Robots and System, (2010), 5060-5066.
11) G. Paschew, A. Richter, High-resolution tactile display operated by an integrated Smart Hydrogel actuator array, Proc. SPIE, 7642, (2010), 1-8.
12) H.S. Lee, D.H. Lee, D.G. Kim, U.K. Kim, C.H. Lee, N.N. Linh, N.C. Toan, J.C. Koo, H. Moon, A.D. Nam, J. Han, H.R. Choi, Tactile display with rigid coupling, Electroact. Polym. Actuat. Dev. 2012, (2012), 83400E-1-9.
13) T. Maeno, K. Otokawa, M. Konyo, Tactile display of surface texture by use of amplitude modulation of ultrasonic vibration, in: Proceedings of 2006 IEEE Ultrasonics Symposium, (2006), 62-65.

14) S. Asano, S. Okamoto, Y. Matuura, H. Nagano, Y. Yamada, Vibrotactile display approach that modify roughness sensations of real texture, in: Proceedings of the 21st IEEE International Symposium on Robot and Human Interactive Communication, (2012), 1001-1006.
15) H. Kajimoto, Electro-tactile display with real-time impedance feedback using pulse width modulation, IEEE Trans. Haptics, 5 (2), (2012), 184-188.
16) C.H. Lee, M.G. Jang, Virtual surface characteristics of a tactile display using magneto-rheological fluids, Sensors, 11 (3), (2011), 2845-2856.
17) Y. Kim, I. Oakley, J. Ryu, Design and psychophysical evaluation of pneumatic tactile display, in: Proceedings of SICE-ICASE International Joint Conference 2006, (2006), 1933-1988.
18) T. Hachisu, M. Fukumoto, Vacuum Touch: attractive force feedback interface for haptic interactive surface using air suction, in: Proceedings of CHI 2014, (2014), 411-420.
19) X. Wu, S.H. Kim, H. Zhu, C.H. Ji, G. Mark, A refreshable braille cell based on pneumatic micro-bubble actuators, J. Microelectromech. Syst. 21 (4), (2012), 908-916.
20) L. Santos-Carreras, K. Leuenberger, P. Retornaz, R. Gassert, H. Bleuler, Design and psychophysical evaluation of a tactile pulse display for tele-operated artery palpation, in: Proceedings of the 2010 IEEE/RSJ International Conference on Intelligent Robots and System, (2010), 5060-5066.
21) P. Smithmaitrie, J. Kanjantoe, P. Tandayya, Touching force response of the piezoelectric braille cell, Disabil. Rehabil. Assist. Technol. 3 (14), (2008), 360-365.
22) S. Soulimane, M.A. Nigassa, B. Bouazza, H. Camon, Micro-actuator modeling to develop a new template for the Braille, in: Proceedings of 15th International Conference on Thermal Mechanical and Multi-Physics and Experiments in Microelectronics and Microsystem, (2014), 1-3.